J. Fluid Mech. (1981), *vol.* 109, *pp.* 339–348
Printed in Great Britain

Linear growth rates for the Rayleigh–Bénard instability in cylindrical geometry

By J. N. SHAUMEYER, R. P. BEHRINGER AND RALPH BAIERLEIN

Department of Physics, Wesleyan University, Middletown, Connecticut 06457 U.S.A.

(Received 13 August 1979 and in revised form 17 November 1980)

We report theoretical growth rates for the Rayleigh–Bénard instability when the fluid layer is contained by non-slip walls in a cylindrical geometry with diameter D and height L. Our results are for the growth rates of the first two axisymmetric modes as functions of the Prandtl number P and the aspect ratio $\gamma \equiv D/2L$. We have considered the two extreme cases of ideally insulating and ideally conducting side walls, and found that the growth rate is relatively insensitive to the choice of the thermal boundary conditions on the side walls. Our results are useful in understanding recent experimental measurements of the convective time-scale.

1. Introduction

When a layer of fluid is heated from below, Rayleigh–Bénard convection will occur if the temperature difference ΔT across the layer exceeds a critical value ΔT_c. The walls containing the fluid can significantly affect the convecting state, and wall effects have been the subject of a number of recent theoretical studies. These include work by Davis (1967), Liang, Vidal & Acrivos (1969), Charlson and Sani (1970, 1971, 1975), Daniels (1977, 1978), Hall & Walton (1977), Brown & Stewartson (1978) and Stewartson & Weinstein (1979). There have also been several experimental studies by Rossby (1969), Krishnamurti (1970), Koschmieder (1974), Koschmieder & Pallas (1974), Ahlers (1975) and Bergé & Dubois (1974), which provide detailed information on the steady-state properties of the convective state. More recently, a number of experimenters, including Behringer & Ahlers (1977), Wesfreid *et al.* (1978) and Ahlers *et al.* (1980) have studied the time-development of steady convection.

The time-scale for establishing the convective state is set by the linear growth rate σ through the appropriate amplitude equation, an idea first developed by Segel (1969) and Newell & Whitehead (1969). The parameter σ has only been obtained for a few special cases. For instance, Davey (1962) has calculated σ for $P = 1$ for an infinite fluid layer with non-slip horizontal boundaries. (The Prandtl number P is defined below.) Behringer & Ahlers (1977) and Wesfreid *et al.* (1978) have calculated σ for the same boundary conditions but for all Prandtl numbers. To our knowledge, no detailed calculations of σ have been made for moderate size geometries, with the experimentally relevant conditions of both horizontal and vertical rigid non-slip walls. Recent improvements in experimental technique seem to warrant such calculations. Accordingly, the object of this paper is to provide values of σ appropriate to experiments done in cylindrical geometries for a large range of aspect ratios γ. Here γ is defined as the

ratio $D/2L$ with L the height of the fluid layer and D its diameter. In particular, we wish to address the experimental observation by Behringer & Ahlers (1977), who used fairly small containers ($\gamma = 2{\cdot}08$ and $4{\cdot}72$), that the convective time-scale seems to vary rather slowly with aspect ratio. In addition, model calculations by Brown & Stewartson (1978) indicate that both the first and second radial modes contribute to the convective state. Accordingly we present results for both cases. Koschmieder's (1974) visual observations of convection in cylindrical containers indicate that the flows are axisymmetric and take the form of toroidal rolls centred on the cylinder axis. Although there is some evidence (Ahlers *et al.* 1980) that under the appropriate conditions straight rolls and hexagons in a cylinder may be important, we present results only for axisymmetric flows.

2. Mathematical framework

We specify cylindrical symmetry by writing a dimensionless velocity field $\mathbf{U}$ as

$$\mathbf{U} \equiv (L/\kappa R^{\frac{1}{2}})\,\mathbf{v} = -L^2 \operatorname{curl}\left[\frac{\Psi(r,z,t)\,\hat{\boldsymbol{\phi}}}{\gamma}\right] \tag{1}$$

and a dimensionless temperature field Θ as

$$\Theta \Delta T \equiv T(r,z,t) - [T_{\text{lower}} - (z/L)\,\Delta T]. \tag{2}$$

Here $\mathbf{v}$ is the physical velocity, L is the fluid (or container) height, κ is the thermal diffusivity, R is the Rayleigh number, Ψ is the stream function and $\hat{\boldsymbol{\phi}}$ is an azimuthal unit vector in cylindrical co-ordinates. The temperature T is assumed to be independent of r at the lower horizontal boundary where it has the value T_{lower}, and at the upper horizontal boundary where it has the value $T_{\text{lower}} - \Delta T$. The Rayleigh number is defined conventionally as $R \equiv g\alpha L^3 \Delta T/\kappa\nu$, where g is the acceleration of gravity, α the isobaric expansion coefficient and ν the kinematic viscosity. The use of $R^{-\frac{1}{2}}$ in equation (1) provides a useful although not essential scale factor. The remaining global parameters for the system are the Prandtl number $P \equiv \nu/\kappa$ and the aspect ratio γ.

While the convection is still in the linear domain, each mode, which has both temperature and velocity parts, responds as $\exp(\sigma \tilde{t})$, where $\tilde{t} \equiv t\kappa/L^2$ is the dimensionless time. The growth rates σ are real, as shown for instance by Schlüter, Lortz & Busse (1965), and depend on R, P and γ. Of particular interest is the Rayleigh number R_n at which the nth mode growth rate σ_n is zero. Values of R_n have been previously computed by Charlston & Sani (1970, 1971) for both axisymmetric and non-axisymmetric modes.

We have extended the variational principle of Charlson & Sani to the calculation of the growth rate. The functional we need is

$$I[\theta, \psi; \sigma, R^{\frac{1}{2}}, P] \equiv 2R^{\frac{1}{2}}\langle \theta \mathbf{u} \,.\, \hat{\mathbf{z}} \rangle - \langle L^2[\partial_i \theta\, \partial_i \theta + \partial_i u_j\, \partial_i u_j] + \sigma[\theta^2 + P^{-1}\mathbf{u}\,.\,\mathbf{u}] \rangle, \tag{3}$$

where $\theta(r,z) \equiv \Theta/e^{\sigma \tilde{t}}$, $\psi(r,z) \equiv \Psi/e^{\sigma \tilde{t}}$, and $\mathbf{u}(r,z) \equiv \mathbf{U}/e^{\sigma \tilde{t}}$. Angular brackets denote an average over the cylindrical volume. Varying I with respect to θ generates the heat equation, while varying with respect to ψ generates the curl of the Navier–Stokes equation, both in the linearized form of the Boussinesq approximation in the absence of steady convection and given the previous specification of exponential time dependence. These equations are discussed in detail by Chandrasekhar (1961), and Charlson & Sani (1970). The requisite boundary conditions are these: (1) to implement a non-slip

constraint on the velocity, both ψ and grad ψ must vanish on all surfaces; (2) the function θ must vanish on the horizontal surfaces, corresponding to experimentally fixed temperature at those surfaces; (3) the product $\theta\,\partial\theta/\partial r$ must vanish on the vertical walls. Insulating walls imply the constraint $\partial\theta/\partial r = 0$ at $r = \gamma L$, whereas conducting walls are represented by $\theta = 0$ at $r = \gamma L$. For a real experiment, the actual conditions on θ at the fluid–side-wall interface are that θ be continuous and that the heat current also be continuous. Additional conditions must be applied at the outer radius of the walls. Since such an exact treatment of the thermal boundary conditions is neither computationally practical nor general to all experiments, we have chosen the two extreme cases above. In the results which follow, we show that the growth rate depends very little on the choice of thermal conditions for $\gamma \gtrsim 1$.

In choosing trial functions for the variational problem, we follow Charlson & Sani (1970) and adopt the forms

$$\psi(r,z) = \Sigma B_{km} Y_k(r/\gamma L)\, X_m(z/L), \tag{4}$$

$$\theta(r,z) = \Sigma A_{ij} J_0(\alpha_i r/\gamma L) \sin(j\pi z/L). \tag{5}$$

The eigenvalue α_i in the Bessel function $J_0(\alpha_i r/\gamma L)$ is chosen to meet the boundary conditions at $r = \gamma L$, namely that either J_0 or J_0' vanish there. One can expect the first relevant modes to be symmetric about the midplane; hence the integer j in the sine function can be restricted to odd integers.

The radial function Y_k is specified by the differential equation

$$\left[\rho \frac{d}{d\rho}\left(\frac{1}{\rho}\frac{d}{d\rho}\right)\right]^2 Y_k(\rho) = \xi_k^4 Y_k(\rho), \tag{6}$$

where $\rho \equiv r/\gamma L$, so that the range of ρ is $0 \leqslant \rho \leqslant 1$. The quantity ξ_k is an eigenvalue of this fourth-order equation. The boundary conditions on Y_k follow from the use of Y_k in the stream function ψ. The vanishing of ψ and grad ψ at the walls requires

$$Y_k(1) = Y_k'(1) = 0. \tag{7}$$

A finite value for $\mathbf{u}\cdot\hat{\mathbf{z}}$ as one approaches the axis implies

$$\lim_{\rho\to 0} \frac{1}{\rho} Y_k'(\rho) = \text{finite number}. \tag{8}$$

Continuity of the horizontal portion of $\mathbf{u}$ for arbitrary approach to the axis requires

$$\lim_{\rho\to 0} \frac{1}{\rho} Y_k(\rho) = 0. \tag{9}$$

The axial function X_m is most easily developed with an independent variable that is zero at the midplane; let

$$\zeta \equiv (z/L) - \tfrac{1}{2}, \quad \tilde{X}_m(\zeta) \equiv X_m(z/L), \tag{10}$$

where ζ has the range $-\frac{1}{2} \leqslant \zeta \leqslant \frac{1}{2}$. The differential equation for X_m is simply

$$d^4\tilde{X}_m/d\zeta^4 = \delta_m^4 \tilde{X}_m, \tag{11}$$

where δ_m is an eigenvalue. The boundary conditions are that

$$\tilde{X}_m(\pm\tfrac{1}{2}) = \tilde{X}'_m(\pm\tfrac{1}{2}) = 0. \tag{12}$$

Solutions to equation (11) have been discussed at some length by Chandrasekhar (1961, appendix v and references therein). The remaining functions and their eigenvalues as well as useful overlap integrals have been tabulated by the authors and are available on request.

3. The growth rate derivative

Substituting the trial functions into (3) and then varying with respect to the expansion coefficients $\{A_{ij}, B_{km}\}$ generates two homogeneous matrix equations. If a non-zero solution for the expansion coefficients is to exist, the determinant D of the combined matrix coefficients must vanish:

$$D(\sigma, R, P, \gamma) = 0. \tag{13}$$

The critical Rayleigh number $R_c = R_1$ is determined as the lowest R for which $D(0, R, P, \gamma) = 0$ holds; R_2 is the next lowest Rayleigh number which satisfies this condition for an axisymmetric mode. When σ is set to zero, the functional I no longer depends on P, and so the R_n are independent of the Prandtl number.

Of most use are the growth rate derivatives (at threshold),

$$\frac{d\sigma_n}{d\epsilon} = \frac{d\sigma_n}{dR} R_n, \tag{14}$$

where $\epsilon \equiv (R - R_n)\, R_n$, and is understood to depend on the R_n for the appropriate mode. We calculated that derivative by numerically solving $D(\Delta\sigma_n, R, P, \gamma) = 0$ for $R = R_n + \Delta R$, given a prescribed small $\Delta\sigma_n$, typically 10^{-2}.

The dependence of $d\sigma_n/d\epsilon$ on the Prandtl number can be deduced from the functional I and the ensuing structure of D. Equivalently one can reason from the functional as follows. Let $[\theta_n, \psi_n]$ denote the fields that give the stationary value at $\sigma_n = 0, R^{\frac{1}{2}} = R_n^{\frac{1}{2}}$. The fields $[\theta_n + \Delta\theta, \psi_n + \Delta\psi]$ are to do the same at $\sigma_n = \Delta\sigma_n$, $R^{\frac{1}{2}} = R_n^{\frac{1}{2}} + \Delta(R^{\frac{1}{2}})$. Now consider the difference of the two functionals. The property that $[\theta_n, \psi_n]$ provide an extremum enables one to eliminate those linear infinitesimal terms that contain $\Delta\theta$ and $\Delta\psi$. The result is

$$\begin{aligned} I[\theta_n + \Delta\theta, \psi_n + \Delta\psi; \Delta\sigma_n, R_n^{\frac{1}{2}} + \Delta(R^{\frac{1}{2}}), P] - I[\theta_n, \psi_n; 0, R_n^{\frac{1}{2}}, P] \\ = \Delta(R^{\frac{1}{2}})\, 2\langle \theta_n \mathbf{u}_n . \hat{\mathbf{z}} \rangle - \Delta\sigma_n \langle \theta_n^2 + P^{-1} |\mathbf{u}_n|^2 \rangle + O(\Delta^2). \end{aligned} \tag{15}$$

Moreover, the equations of motion themselves imply that $I = 0$ at its stationary value, and so the left-hand side of (15) is zero. Dividing through by $\Delta(R^{\frac{1}{2}})$ and passing to the limit, one finds

$$\begin{aligned} \frac{d\sigma_n}{d\epsilon} &= \lim \frac{\Delta\sigma_n}{\Delta(R^{\frac{1}{2}})} \frac{\Delta(R^{\frac{1}{2}})}{\Delta\epsilon} \\ &= \frac{\langle \theta_n \mathbf{u}_n . \hat{\mathbf{z}} \rangle\, R_n^{\frac{1}{2}}}{\langle \theta_n^2 \rangle + P^{-1} \langle |\mathbf{u}_n|^2 \rangle} \end{aligned} \tag{16}$$

$$= \frac{\langle \partial_i \theta_n \partial_i \theta_n + \partial_i u_{nj} \partial_i u_{nj} \rangle (\frac{1}{2}L^2)}{\langle \theta_n^2 \rangle + P^{-1} \langle |\mathbf{u}_n|^2 \rangle}, \tag{17}$$

after $I = 0$ has been invoked to eliminate R_n. The dependence of the growth rate derivative on P is delightfully simple. We note that Joseph (1976) obtained a similar result for a more complex problem. We have presented the above proof to provide a simple derivation obtainable within the context of the preceding discussion.

We tabulate $d\sigma_n/d\epsilon$ for $n = 1$ and 2, both with $P = 1$ and ∞. The value of the derivative at any other Prandtl number can be computed readily from the exact interpolation formula derivable from equation (17):

$$[d\sigma_n/d\epsilon]^{-1} = [(d\sigma_n/d\epsilon)_\infty]^{-1} \left\{ 1 + \frac{1}{P} \left[\frac{(d\sigma_n/d\epsilon)_\infty}{(d\sigma_n/d\epsilon)_1} - 1 \right] \right\}. \tag{18}$$

Our experience indicates that the tabulated growth rate derivatives are numerically reliable to 0·2 %. Computations for the tables were done with the first three symmetric axial trial functions ($j = 1, 3, 5$) and with eight radial trial functions. As the aspect ratio was increased, the chosen set of radial functions was shifted toward higher spatial frequency. The values of R_1 and R_2 so calculated typically agree with Charlson & Sani (1971) to within 0·02 % over their range $1 \leqslant \gamma \leqslant 8$. Nowhere do the two calculations differ by more than 0·07 %, although Charlson & Sani typically used ten radial trial functions. (As far as R_n is concerned, of course, we simply repeated their method, but computational limitations restricted us to fewer trial functions.) In a few instances, we calculated $d\sigma_n/d\epsilon$ a second way: we solved the matrix equations for the expansion coefficients $\{A_{tj}, B_{km}\}$ at R_n and then evaluated the volume averages in (16). Using the same trial function, we found agreement on the derivative to better than 0·02 %. We have also done several calculations with 10 radial trial functions and found agreement to within 0·2 %.

4. Discussion

The results of our calculations are presented in table 1 and figures 1, 2, and 3. (Although we calculated the growth rate derivative through $\gamma = 16$, the variation in the derivative is no more than 1 % for $\gamma > 10$, so only values for $\gamma \leqslant 10$ are given in the table.) The Rayleigh numbers are not given here, as they may be obtained from Charlson & Sani (1970). The graph in figure 1 displays $d\sigma_1/d\epsilon$ when $P = 1$ and the walls are insulating. Similarly, figure 2 shows $d\sigma_1/d\epsilon$ when $P = 1$ with conducting walls. Figure 1 is typical of all cases and will serve as a point of departure. Three features are noteworthy. First, there is relatively little change, no more than 10 %, in $d\sigma_n/d\epsilon$ with γ until γ is smaller than roughly 2·0. Second, $d\sigma_n/d\epsilon$ is very insensitive to the thermal boundary conditions. For instance, when $P = 1{\cdot}0$, $d\sigma_1/d\epsilon$ for the cases of insulating and conducting walls differ by no more than 8 % for γ as low as 0·75. This is particularly useful, since an exact accounting of the true experimental conditions is generally rather difficult. Our results help explain why Behringer & Ahlers (1977) obtained, within the experimental scatter of 20 %, the same growth rate for $\gamma = 2{\cdot}08$ and $\gamma = 4{\cdot}72$, and a growth rate value which was experimentally indistinguishable from the infinite aspect ratio prediction. The third notable feature is the oscillations in $d\sigma_n/d\epsilon$ versus γ. The relative minima in $d\sigma_n/d\epsilon$ correlate well with relative maxima

	Insulating			Conducting		
γ	$(d\sigma_1/d\epsilon)_\infty$	$(d\sigma_2/d\epsilon)_1$	$(d\sigma_2/d\epsilon)_\infty$	$(d\sigma_1/d\epsilon)_\infty$	$(d\sigma_2/d\epsilon)_1$	$(d\sigma_2/d\epsilon)_\infty$
1·00	25·66	34·52	57·93	25·92	30·27	46·86
1·25	20·27	24·59	40·45	22·25	22·95	36·41
1·50	17·71	18·96	30·03	20·53	18·46	29·16
1·75	19·12	13·66	19·79	20·55	15·35	23·52
2·00	22·13	11·08	15·32	20·96	14·26	21·39
2·25	20·33	16·21	25·42	20·48	15·00	22·85
2·50	18·91	16·06	25·40	19·95	14·97	23·08
2·75	19·10	13·90	20·94	19·90	14·10	21·47
3·00	20·80	12·01	17·30	20·17	13·47	20·24
3·25	20·17	13·33	19·94	20·08	13·71	20·72
3·50	19·31	14·78	23·08	19·80	13·96	21·32
3·75	19·27	13·75	20·92	19·77	13·62	20·71
4·00	20·24	12·49	18·38	19·93	13·25	19·95
4·25	20·04	12·93	19·28	19·89	13·41	20·29
4·50	19·49	14·10	21·78	19·73	13·58	20·67
4·75	19·38	13·60	20·72	19·71	13·39	20·31
5·00	19·99	12·73	18·94	19·85	13·15	19·82
5·25	19·94	12·91	19·31	19·81	13·31	20·15
5·50	19·57	13·73	21·05	19·67	13·42	20·41
5·75	19·46	13·47	20·52	19·69	13·25	20·07
6·00	19·86	12·85	19·24	19·81	13·08	19·73
6·25	19·87	12·81	19·16	19·75	13·26	20·09
6·50	19·62	13·51	20·64	19·66	13·33	20·27
6·75	19·50	13·37	20·36	19·69	13·17	19·93
7·00	19·80	12·92	19·40	19·78	13·04	19·66
7·25	19·82	12·85	19·26	19·72	13·21	20·02
7·50	19·64	13·29	20·20	19·66	13·28	20·17
7·75	19·54	13·30	20·23	19·66	13·12	19·86
8·00	19·75	12·95	19·50	19·75	13·01	19·62
8·25	19·79	12·87	19·33	19·71	13·17	19·95
8·50	19·65	13·20	20·04	19·65	13·24	20·10
8·75	19·56	13·27	20·18	19·68	13·10	19·82
9·00	19·73	13·02	19·64	19·74	12·99	19·61
9·25	19·77	12·87	19·34	19·69	13·08	19·77
9·50	19·65	13·15	19·93	19·65	13·16	19·94
9·75	19·58	13·23	20·09	19·68	13·08	19·79
10·00	19·71	13·03	19·67	19·74	13·00	19·59

TABLE 1. The growth rate derivative $d\sigma_n/d\epsilon$ associated with the first and second modes ($n = 1, 2$), for the cases $P = \infty$, and $P \simeq 1$ and ∞ respectively, as a function of aspect ratio γ. Values for both insulating vertical walls and conducting vertical walls are given. Results for $n = 1$, $P = 1$ are shown in figures 1 and 2.

in R_n and with changes, as γ increases, to patterns with one additional roll. For example, as shown in figure 3, the minimum of $d\sigma_1/d\epsilon$ in the vicinity of $\gamma = 2{\cdot}6$ precedes the respective maximum in R_1 by about 0·2 in aspect ratio. Charlson & Sani (1970) give the aspect ratio at which roll changes occur (to within $\pm 0{\cdot}13$) for aspect ratios up to $\gamma = 8$; in all those instances, the minimum in $d\sigma_1/d\epsilon$ lies within or just below the transition region.

One can understand the oscillations intuitively. When the aspect ratio is centred between transition points in the roll pattern, the rolls are reasonably uniform in cross-

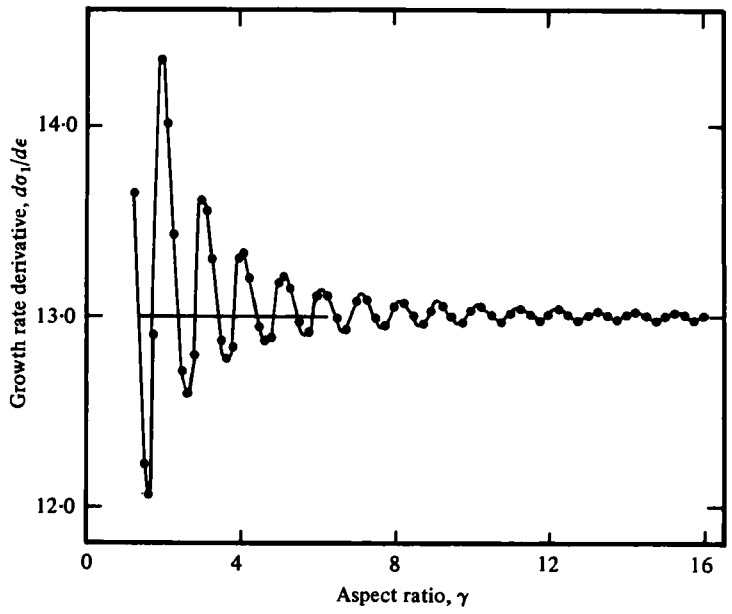

FIGURE 1. The growth rate derivative $d\sigma_1/d\epsilon$ as a function of the aspect ratio γ for insulating vertical walls and $P = 1$. The behaviour at the relative maxima and minima is smooth, as demonstrated by auxillary calculations in steps of $\Delta\gamma = 0{\cdot}05$ near $\gamma = 2{\cdot}6$, $4{\cdot}05$, and $4{\cdot}65$. The horizontal bar is the value of $d\sigma/d\epsilon$ at $P = 1$ and $\gamma = \infty$, as calculated by Behringer & Ahlers (1977).

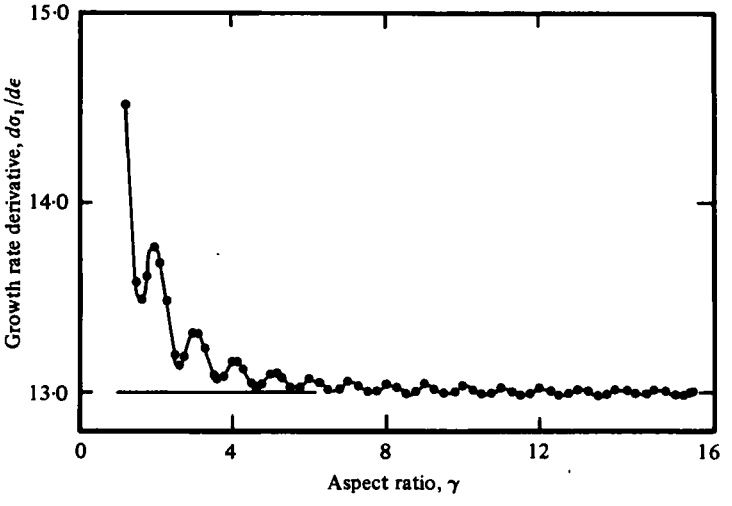

FIGURE 2. The growth rate derivative $d\sigma_1/d\epsilon$ as a function of aspect ratio γ for conducting vertical walls and $P = 1$. The horizontal bar is the value given by Behringer & Ahlers (1977) for $\gamma = \infty$.

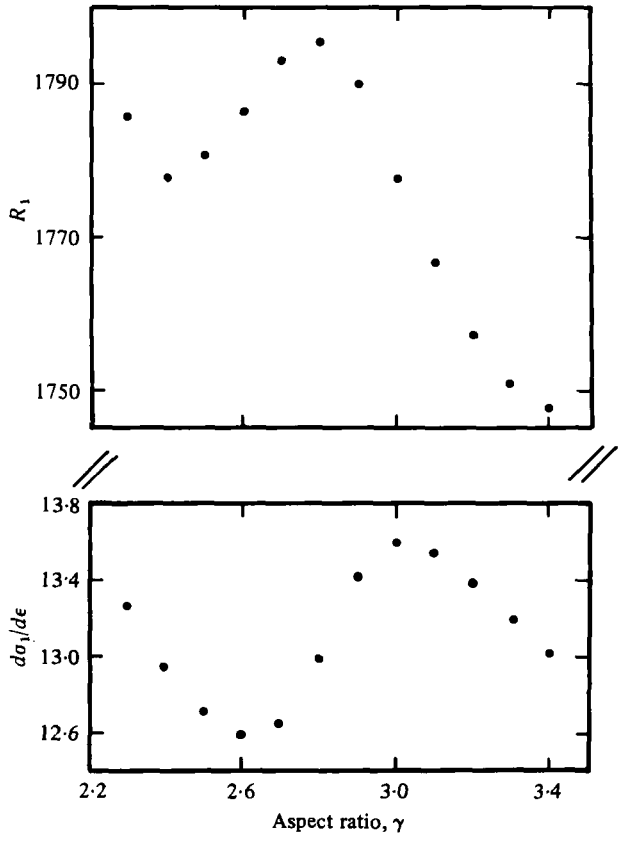

FIGURE 3. Comparison of relative extrema in R_1 (top) and $d\sigma_1/d\epsilon$ (bottom), over the range $2{\cdot}3 \leqslant \gamma \leqslant 3{\cdot}4$, which includes the transition from 2 to 3 rolls. The calculations were done for $P = 1$, with insulating vertical walls.

section as one goes from axis to walls. Near transition points, however, the outermost roll or two have an anomalous structure: wider or more narrow than usual. These anomalous rolls have a structure that is perturbed from the smooth infinite aspect ratio planform because of the side walls. One would expect the system to establish the less-than-optimum structure less readily than the uniform rolls. The growth rate derivative should be relatively small and the onset Rayleigh number relatively large as our calculations indicate.

As γ grows large, the oscillations in $d\sigma_1/d\epsilon$ converge toward the value appropriate for infinite aspect ratio, as computed from the expression given by Behringer & Ahlers (1977). From equation (17), one can understand why the oscillations must diminish in magnitude. As γ increases there is a relatively smaller contribution to the volume averages from the region near the walls. The roll structure near the walls must have progressively less influence on $d\sigma_n/d\epsilon$, and so that quantity must show progressively less variation with aspect ratio. The theoretical expression, equation (17), also indicates why $d\sigma_n/d\epsilon$ is insensitive to the thermal boundary conditions. Provided γ is substantially greater than unity, the volume averages are not sensitive to the boundary conditions on the temperature field θ at the walls.

A few words should be said about roll patterns that are not axisymmetric. Charlson

& Sani (1971) computed the Rayleigh number at which states with one to five full cycles in azimuthal variation become unstable. Once the aspect ratio exceeds three or so, there is always some such state with critical Rayleigh number within 1 % of the marginal number for the axisymmetric state. Moreover, there are aspect ratios at which a non-axisymmetric state becomes unstable at a lower Rayleigh number than does the axisymmetric state. Thus it would be useful, in principle, to compute the growth rate derivative for the first few states with azimuthal variation.

Here we note only that, when the marginal Rayleigh numbers differ little from that for the axisymmetric state, the growth rate derivative will, we expect, also differ little. The integral expression in (16) provides the basis for this belief. Although relations (16) and (17) were derived from the variational principle with axisymmetry specified, they also follow directly from the linearized Navier–Stokes and heat equations without any symmetry assumption. The correlation between $\theta \mathbf{u} \cdot \hat{\mathbf{z}}$ that appears in the numerator of (16) should not be sensitive to a change in symmetry. The denominator is essentially a normalizing factor. Thus, whenever R_n changes little, one can expect $d\sigma_n/d\epsilon$ to follow suit. For support, one can note the situation at infinite aspect ratio; in the Boussinesq approximation, the growth rate derivative is independent of the azimuthal dependence of the mode.

5. Summary

We have calculated the growth rate for the first two radially symmetric convective modes in cylindrical geometry. Our results explain the experimental observation of Behringer & Ahlers (1977) that σ seems to depend at best weakly on aspect ratio for $\gamma \gtrsim 2$. We find relatively little dependence of σ on the thermal boundary conditions at the side walls for $\gamma \geqslant 0{\cdot}75$. This result is particularly useful, since exact experimental thermal boundary conditions are rather difficult to implement.

Thanks for hospitality go to Professor Ronald Ruby and the Physics Board at the University of California, Santa Cruz, where R. B.'s portion of this paper was completed during a sabbatical leave. We gratefully acknowledge extensive use of the Wesleyan University and University of California computer facilities.

REFERENCES

AHLERS, G. 1975 In *Fluctuations, Instabilities, and Phase Transitions* (ed. T. Riste). Plenum.
AHLERS, G., CROSS, M. C., HOHENBERG, P. C. & SAFRAN, S. 1980 *J. Fluid Mech.* (to appear).
BEHRINGER, R. P. & AHLERS, G. 1977 *Phys. Lett.* A **62**, 329.
BERGÉ, P. & DUBOIS, M. 1974 *Phys. Rev. Lett.* **32**, 1041.
BROWN, S. N. & STEWARTSON, K. 1978 *Proc. Roy. Soc.* A **360**, 455.
CHANDRASEKHAR, S. 1961 *Hydrodynamic and Hydromagnetic Stability*. Clarendon.
CHARLSON, G. S. & SANI, R. L. 1970 *J. Heat Mass Transfer* **13**, 1479.
CHARLSON, G. S. & SANI, R. L. 1971 *J. Heat Mass Transfer* **14**, 2157.
CHARLSON, G. S. & SANI, R. L. 1975 *J. Fluid Mech.* **71**, 210.
DANIELS, P. G. 1977 *Proc. Roy. Soc.* A **358**, 173.
DANIELS, P. G. 1978 *Mathematika* **25**, 216.
DAVEY, A. 1962 *J. Fluid Mech.* **14**, 336.
DAVIS, S. H. 1967 *J. Fluid Mech.* **30**, 465.

HALL, P. & WALTON, I. C. 1977 *Proc. Roy. Soc.* A **358**, 199.
JOSEPH, D. D. 1976 *Stability of Fluid Motions*. Springer.
KOSCHMIEDER, E. L. 1974 *Adv. Chem. Phys.* **26**, 177.
KOSCHMIEDER, E. L. & PALLAS, S. G. 1974 *J. Heat Mass Transfer* **17**, 991.
KRISHNAMURTI, R. 1970 *J. Fluid Mech.* **42**, 309.
LIANG, S. F., VIDAL, A. & ACRIVOS, A. 1969 *J. Fluid Mech.* **36**, 239.
NEWELL, A. C. & WHITEHEAD, J. A. 1969 *J. Fluid Mech.* **38**, 279.
ROSSBY, H. T. 1969 *J. Fluid Mech.* **36**, 309.
SCHLÜTER, A., LORTZ, D., & BUSSE, F. 1965 *J. Fluid Mech.* **23**, 129.
SEGEL, L. A. 1969 *J. Fluid Mech.* **38**, 203.
STEWARTSON, K. & WEINSTEIN, M. 1979 *Phys. Fluids* **22**, 1421.
WESFREID, J., POMEAU, Y., DUBOIS, M., NORMAND, C. & BERGÉ, P. 1978 *J. Phys. Lett.* **39**, 725.